



Research Paper

Nrf2-regulated redox signaling in brain endothelial cells adapted to physiological oxygen levels: Consequences for sulforaphane mediated protection against hypoxia-reoxygenation

Gabriela Warpsinski, Matthew J. Smith, Salil Srivastava¹, Thomas P. Keeley², Richard C. M. Siow, Paul A. Fraser, Giovanni E. Mann^{*}

King's British Heart Foundation Centre for Research Excellence, School of Cardiovascular Medicine & Sciences, Faculty of Life Sciences & Medicine, King's College London, 150 Stamford Street, London, SE1 9NH, UK

ARTICLE INFO

Keywords:

Brain endothelial cells
Keap1-Nrf2
Heme oxygenase-1
Glutamate cysteine ligase
Ischemia-reoxygenation
Redox signaling
Sulforaphane
Oxygen
Physiological normoxia

ABSTRACT

Ischemic stroke is associated with a surge in reactive oxygen species generation during reperfusion. The narrow therapeutic window for the delivery of intravenous thrombolysis and endovascular thrombectomy limits therapeutic options for patients. Thus, understanding the mechanisms regulating neurovascular redox defenses are key for improved clinical translation. Our previous studies in a rodent model of ischemic stroke established that activation of Nrf2 defense enzymes by pretreatment with sulforaphane (SFN) affords protection against neurovascular and neurological deficits. We here further investigate SFN mediated protection in mouse brain microvascular endothelial cells (bEnd.3) adapted long-term (5 days) to hyperoxic (18 kPa) and normoxic (5 kPa) O₂ levels. Using an O₂-sensitive phosphorescent nanoparticle probe, we measured an intracellular O₂ level of 3.4 ± 0.1 kPa in bEnd.3 cells cultured under 5 kPa O₂. Induction of HO-1 and GCLM by SFN (2.5 μM) was significantly attenuated in cells adapted to 5 kPa O₂, despite nuclear accumulation of Nrf2. To simulate ischemic stroke, bEnd.3 cells were adapted to 18 or 5 kPa O₂ and subjected to hypoxia (1 kPa O₂, 1 h) and reoxygenation. In cells adapted to 18 kPa O₂, reoxygenation induced free radical generation was abrogated by PEG-SOD and significantly attenuated by pretreatment with SFN (2.5 μM). Silencing Nrf2 transcription abrogated HO-1 and NQO1 induction and led to a significant increase in reoxygenation induced free radical generation. Notably, reoxygenation induced oxidative stress, assayed using the luminescence probe L-012 and fluorescence probes MitoSOX™ Red and FeRhoNox™-1, was diminished in cells cultured under 5 kPa O₂, indicating an altered redox phenotype in brain microvascular cells adapted to physiological normoxia. As redox and other intracellular signaling pathways are critically affected by O₂, the development of antioxidant therapies targeting the Keap1-Nrf2 defense pathway in treatment of ischemia-reperfusion injury in stroke, coronary and renal disease will require *in vitro* studies conducted under well-defined O₂ levels.

1. Introduction

Ischemic stroke is a leading cause of death and adult morbidity worldwide [1]. The critical reduction of blood flow within a major cerebral artery leads to reduced oxygen and nutrient delivery to the brain [2], time-dependent neuronal cell death and the development of neurological deficits [3]. The initiation of a pathophysiological cascade, involving oxidative stress and inflammation [4], is further exacerbated

by the generation of reactive oxygen species (ROS) and mitochondrial dysfunction during reperfusion [5,6]. Timely restoration of cerebral blood flow is currently the only effective pharmacological treatment for acute ischemic stroke. Treatment with tissue plasminogen activator (rt-PA) improves reperfusion and functional outcomes, yet is limited to a ~4.5 h window after the onset of stroke due to an increased risk of hemorrhagic transformation [7,8]. Recent trials of endovascular thrombectomy in stroke patients with large vessel occlusion report significant

* Corresponding author.

E-mail address: giovanni.mann@kcl.ac.uk (G.E. Mann).

¹ Respiratory Disease Area, Novartis Institutes for BioMedical Research, Inc. 700 Main Street, Cambridge, MA, 02139, USA.

² Target Discovery Institute, Nuffield Department of Medicine, University of Oxford, Oxford OX3 7FZ, UK.

<https://doi.org/10.1016/j.redox.2020.101708>

Received 28 July 2020; Received in revised form 21 August 2020; Accepted 27 August 2020

Available online 8 September 2020

2213-2317/© 2020 The Author(s). Published by Elsevier B.V. This is an open access article under the CC BY license (<http://creativecommons.org/licenses/by/4.0/>).

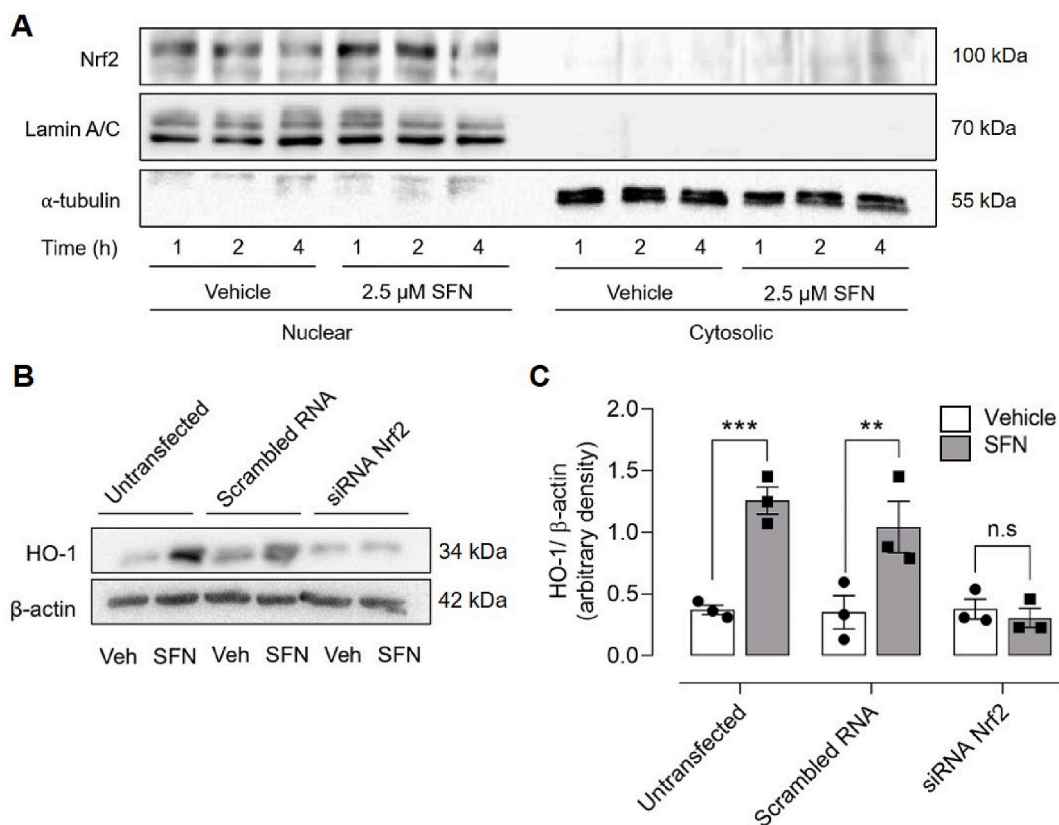


Fig. 1. Silencing Nrf2 abrogates induction of HO-1 by sulforaphane in bEnd.3 endothelial cells

(A) Representative immunoblot of Nrf2 in nuclear and cytosolic fractions isolated from bEnd.3 cells treated for 1, 2 and 4 h with vehicle (0.01% DMSO) or sulforaphane (SFN, 2.5 μ M). Lamin A/C and α -tubulin are loading controls for nuclear and cytosolic fractions, respectively. (B–C) bEnd.3 cells were transfected with scrambled or Nrf2 siRNA 24 h post-seeding to silence Nrf2 transcriptional activity and then challenged with vehicle (0.01% DMSO) or SFN (2.5 μ M) for 24 h. Cell lysates immunoblotted for HO-1 expression relative β -actin (B) and analysed by densitometry (C). Data denote mean \pm S.E.M., $n = 3$ independent bEnd.3 cultures, two-way ANOVA, ** $P < 0.01$, *** $P < 0.001$, n.s. non-significant.

improvements in functional outcomes [1]. However, increased generation of reactive oxygen species in ischemic brain regions may compromise potentially rescuable penumbral tissue surrounding the infarct core [5,9].

Disruption of the blood-brain barrier (BBB) in ischemic stroke leads to extravasation of blood-borne inflammatory cells and fluid into the brain parenchyma which underlies dysregulation of neurovascular function [10–13]. Our previous studies in a rodent model of ischemic stroke established that pretreatment of animals with the dietary isothiocyanate sulforaphane (SFN) [14], an electrophilic activator of the redox sensitive transcription factor Nuclear factor-erythroid 2 p45-related factor 2 (Nrf2) [15,16], significantly reduces BBB permeability, infarct volume and behavioral deficits [17,18]. Our MRI studies further demonstrated that prophylactic SFN delivery reduced lesion volume, consistent with reduced BBB permeability to IgG and improved neurological outcome [17]. Notably, SFN rapidly enters the brain [19] and upregulates Nrf2 and HO-1 expression in brain perivascular astrocytes and endothelial cells [17,18].

The majority of studies in endothelial and other cell types are conducted during culture under atmospheric O_2 (18 kPa), whereas most cells experience much lower levels *in vivo*, with brain endothelial cells exposed to ~ 3 –7 kPa [20]. Hyperoxic conditions create a pro-oxidation environment, reducing replicative lifespan [21] and enhancing cellular antioxidant defenses [22,23], thereby potentially limiting the clinical relevance of *in vitro* findings. We recently reported that SFN mediated induction of select Nrf2 target genes in umbilical vein endothelial cells (HUVEC) is attenuated under physiological normoxia (5 kPa O_2) compared to atmospheric O_2 levels [22]. Moreover, we reported that

adaptation of HUVEC to 5 kPa O_2 enhances nitric oxide bioavailability, modulates agonist-induced Ca^{2+} signaling [24] and protects against Ca^{2+} overload due to increased SERCA activity [25].

In this study, we further explore the mechanisms underlying SFN afforded protection in ischemic stroke by investigating redox signaling in mouse brain microvascular endothelial cells (bEnd.3) subjected to hypoxia-reoxygenation following adaptation to defined O_2 levels. Our findings demonstrate that SFN induces Nrf2-regulated defense enzymes in bEnd.3 cells to protect against reoxygenation induced reactive oxygen species generation. These findings together with our study in of ischemic stroke *in vivo* [17,18] suggest that SFN may be a prophylactic therapeutic for targeting the Keap1-Nrf2 defense pathway in stroke and potentially coronary and renal disease.

2. Methods and materials

2.1. Culture and adaptation of bEnd.3 cells under defined O_2 levels

Endothelialpolyoma middle T antigen transformed mouse brain microvascular endothelial cells (bEnd.3) were obtained from ATCC-LGC (Teddington, UK). Cells were cultured in phenol red free DMEM (Sigma, UK), supplemented with fetal calf serum (10%), L-glutamine (4 mM) and penicillin (100U/ml)/streptomycin (100 μ g/ml). Cell monolayers were maintained for at least 5 days (d) in an O_2 -regulated dual workstation (Scitiver, Baker-Ruskinn, USA), gassed to 18 kPa (hyperoxia), 5 kPa (physiological normoxia) or 1 kPa (hypoxia) O_2 under 5% CO_2 at 37 $^\circ C$. This experimental protocol ensures adaptation of the cell proteome [20] and obviates re-exposure of cells to room air, as all cell culture,

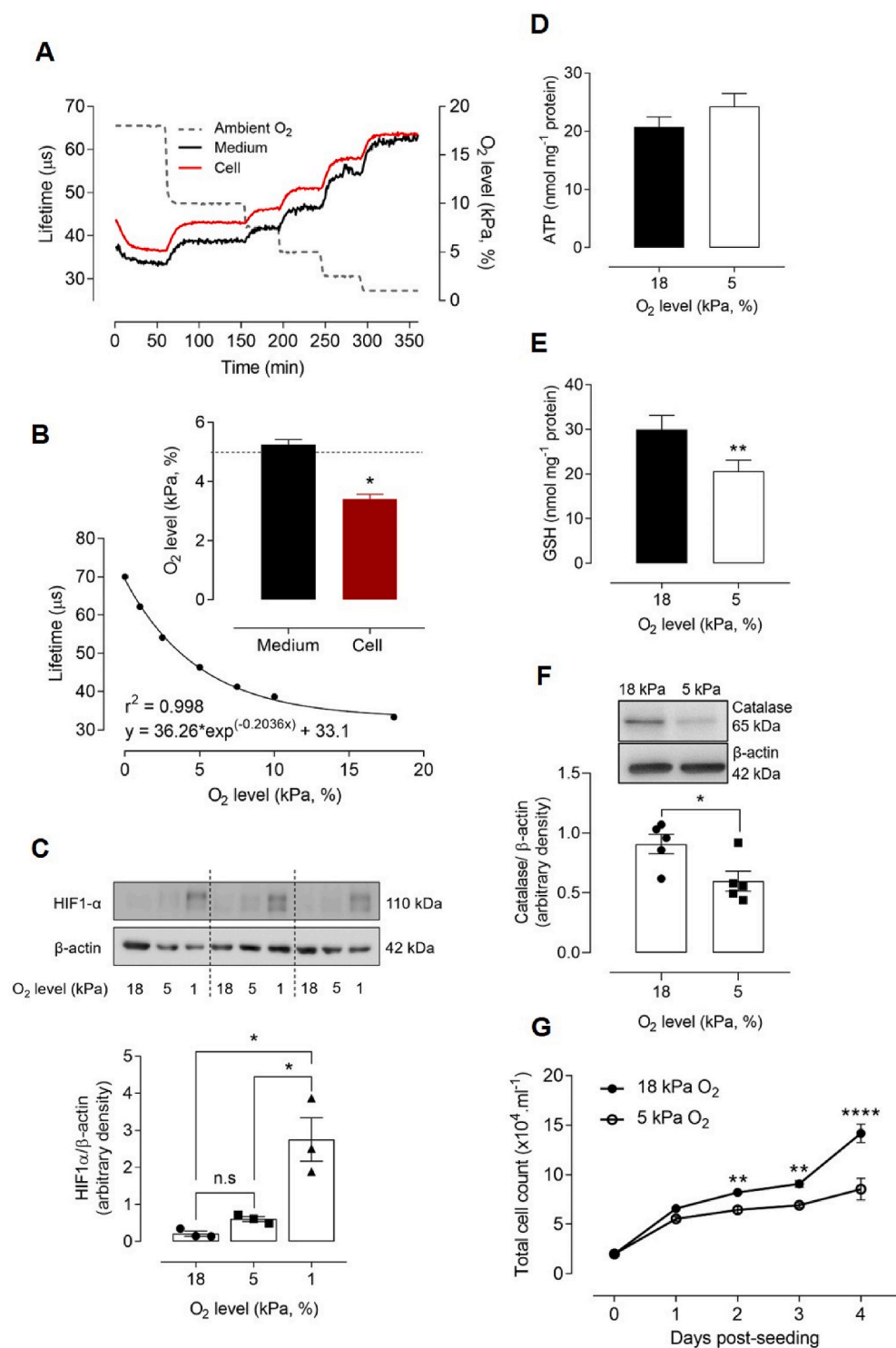


Fig. 2. Adaptation to 5 kPa O_2 alters the redox phenotype of bEnd.3 cells in the absence of HIF-1 α stabilization

bEnd.3 cells adapted to 18 kPa O_2 were loaded with MitoXpress $^{\text{®}}$ -INTRA for 16 h, transferred rapidly to an O_2 -regulated plate reader and exposed to stepwise reductions in O_2 (dotted line, right axis). (A) Phosphorescence lifetime measurements (see Methods) in cells and dissolved O_2 in medium. (B) Averaged phosphorescence lifetime versus ambient O_2 levels in the plate reader were fit by exponential analysis. *Inset*: Interpolated O_2 content in bEnd.3 cell cytosol and medium under 5 kPa O_2 (dashed line). (C) Immunoblots of HIF-1 α expression relative to β -actin and densitometric analysis of 3 cultures (separated by dashed lines). (D–E) Intracellular ATP and GSH levels in cells adapted for 5 d to 18 or 5 kPa O_2 . (F) Immunoblot and densitometric analysis of catalase expression relative to β -actin under 18 or 5 kPa O_2 . (G) Differential rate of bEnd.3 cell proliferation under 18 or 5 kPa O_2 . Data denote mean \pm S.E.M., $n = 3$ –5 independent bEnd.3 cell cultures, * $P < 0.05$, ** $P < 0.01$, **** $P < 0.0001$, n.s. non-significant.

treatments and experiments are conducted within the O_2 -regulated workstation and/or plate reader (CLARIOstar, BMG Labtech, Germany). All experiments were conducted using bEnd.3 cells in passages 7–15.

2.2. Phosphorescence lifetime measurements of O_2 levels in bEnd.3 cell cytosol and medium

Intracellular O_2 levels were monitored in live cells using a cell-penetrating phosphorescent platinum–porphyrin based nanoparticle probe, MitoXpress $^{\text{®}}$ -INTRA (Agilent, USA) [26]. A time-resolved

fluorescence plate reader (CLARIOstar, BMG Labtech), equipped with an atmospheric control unit, enabled us to measure cytosolic O_2 levels under defined ambient O_2 levels. bEnd.3 cells were seeded into 96-well black microtitre plates and loaded with MitoXpress $^{\text{®}}$ -INTRA (10 $\mu\text{g}/\text{ml}$) for 16 h in complete DMEM. The probe emits a phosphorescence signal at 655 ± 55 nm when excited at 355 ± 55 nm [22,24]. Molecular oxygen quenches the phosphorescence signal, and the signal decay is inversely proportional to the concentration of O_2 . Phosphorescence intensity after excitation was measured after 30 μs (t_1) and 70 μs (t_2) with a 30 μs window and converted to probe lifetime (τ) using the formula:

$\tau = (t_2 - t_1) / \ln(f_1/f_2)$, where f_1 and f_2 represent phosphorescence intensities at respective timepoints [27]. Averaged lifetime measured at 7 ambient O_2 tensions was plotted against the known O_2 tension and subjected to an exponential fit analysis. Lifetime values were then interpolated from this curve (see Fig. 2B) to give the dissolved intracellular O_2 level in live bEnd.3 cells. Dissolved O_2 culture medium was also measured in parallel by diluting MitoXpress®-INTRA (2.5 $\mu\text{g}/\text{ml}$) in DMEM medium.

2.3. Immunoblotting

Cell lysates were extracted with SDS lysis buffer containing protease and phosphatase inhibitors (pH 6.8) on ice for 10 min. Denatured samples (10 μg) were separated by gel electrophoresis, electrotransferred onto polyvinylidene difluoride membranes and then probed with primary and HRP-conjugated secondary antibodies, using Lamin A/C (Santa Cruz, USA), α -tubulin (Millipore, UK) or β -actin (Sigma-Aldrich, USA) as reference proteins for nuclear and cell protein, respectively [22,28]. Nuclear protein was extracted using a nuclear extraction kit (Active Motif). Membranes were probed for HO-1 (Cell Signaling Technology), GCLM (gift from Prof. T. Kavanagh, University of Washington, WA, USA), NQO1 (Santa Cruz, USA), HIF-1 α (Abcam, UK), catalase (Calbiochem, UK) and Nrf2 (Santa Cruz, USA). Protein expression was determined by enhanced chemiluminescence with images captured in a gel documentation system (G-BOX, Syngene Ingenius Bioimaging) and analysed by densitometry using Image J software (NIH, USA).

2.4. Quantitative RT-PCR

bEnd.3 cell RNA was isolated using a Nucleospin RNA Kit (Macherey-Nagel) and RNA content and purity assessed using a spectrophotometer (NanoDrop, Thermo Scientific, UK). Total RNA was reverse-transcribed using a high capacity cDNA conversion kit (Applied Biosystems) and HO-1, NQO1, GCLM, Bach1 and Keap1 mRNA assessed by real-time qPCR (Corbett Rotorgene) [22,28] and normalized to the geometric mean of β -2-microglobulin (B2M), ribosomal protein L13a (RPL13A) and succinate dehydrogenase unit complex A (SDHA) (see primer sequences in Supplementary Table S1).

2.5. siRNA Nrf2 silencing

bEnd.3 cells were seeded at 30,000 cells/well and transfected with 40 pmol/well of either scrambled siRNA or Nrf2 siRNA (Santa Cruz, USA) [28] for 24 h using Dharmafect 4 transfection reagent (GE Healthcare, USA), as previously described [29].

2.6. Measurement of intracellular glutathione and ATP levels and cell viability

bEnd.3 cells were adapted to 18 or 5 kPa O_2 for 5 days, and intracellular ATP and GSH extracted using 6.5% trichloroacetic acid (TCA, Sigma, UK). For ATP measurements, extracts were incubated with firefly lantern extract (Sigma, UK) containing both luciferase and luciferin, while total GSH levels were determined using a fluorometric assay [22,30]. Fluorescence and luminescence were measured in a plate reader (CLARIOstar, BMG Labtech). Cell viability was determined assaying mitochondrial dehydrogenase activity with 3-[4,5-dimethylthiazol-2-yl] 2,5-diphenyl tetrazolium bromide (Sigma, UK) [29].

2.7. L-012 luminescence measurements of reactive oxygen species generation

bEnd.3 cells were seeded into white-walled, clear-bottomed 96-well plates and adapted for 5 d under 18 or 5 kPa O_2 . Confluent monolayers were incubated in low-serum medium (1% FCS) for 24 h prior to

incubation in Krebs buffer in the absence or presence of superoxide dismutase (SOD, 100U/ml, Sigma, UK), polyethylene glycol SOD (PSOD, 50U/ml, Sigma, UK), polyethylene glycol catalase (PCAT, 200U/ml, Sigma, UK) or the NADPH oxidase inhibitor VAS2870 (VAS, 5 μM) [31] and the chemiluminescent luminol analogue L-012 (8-amino-5-chloro-7-phenyl-pyridol [3,4-d] pyridazine-1,4-(2H, 3H)dione sodium salt, 10 μM , Wako Chemicals) [32,33]. Cells adapted to either 18 or 5 kPa O_2 were then rapidly (<30 s) transferred to an O_2 -regulated plate reader (CLARIOstar, BMG Labtech) at 37 °C and exposed to hypoxia (1 kPa O_2) for 1 h and reoxygenation under 18 or 5 kPa O_2 , respectively. Luminescence was measured at 60 s intervals over 3 h and data expressed as mean light units/mg protein.

2.8. Mitochondrial reactive oxygen species measured using MitoSOX™ Red

Mitochondrial reactive oxygen species generation was measured using a mitochondrial targeted fluorogenic probe MitoSOX™ Red [34], and we previously confirmed that MitoSOX fluorescence in endothelial cells is attenuated by scavenging superoxide [28,35]. bEnd.3 cells seeded in black-walled, clear-bottomed 96-well plates were cultured under 18 or 5 kPa O_2 for 5 d and then incubated in serum-free DMEM in the absence or presence of rotenone (1 μM , complex 1 inhibitor) or L-NAME (100 μM , eNOS inhibitor). Cells were exposed to hypoxia (1 kPa O_2 , 1 h) and loaded with MitoSOX™ Red (5 μM , Invitrogen) for 5 min before the start of reoxygenation under 18 or 5 kPa O_2 , respectively. Cells were washed twice with ice-cold PBS and fixed with 4% paraformaldehyde for 10 min before staining nuclei with DAPI (2 $\mu\text{g}/\text{ml}$, Sigma). MitoSOX™ Red fluorescence (Ex 545 nm/Em 602 nm) was detected using a Nikon Diaphot microscope, with images captured using an ORCA-03G (Hamamatsu, Japan) camera with 0.89 s exposure. Fluorescence quantification was conducted using image analysis software (ImageJ, NIH, USA), measuring the integrated intensity of fluorescence, area of field of view and mean grey value.

2.9. Intracellular free iron levels in bEnd.3 cells measured using FeRhoNox™-1

Intracellular iron release was measured using FeRhoNox™-1 (Goryo Chemical, Japan), a free iron turn-on fluorescent indicator specific for the detection of labile iron Fe(II) [36,37]. Cells in black, clear-bottomed 96-well plates were adapted to 18 or 5 kPa O_2 and then incubated with FeRhoNox (5 μM) for 1 h, washed twice with PBS and incubated for 30 min with Hank's Balanced Saline Solution (HBSS, Gibco) containing either vehicle (DMSO, 0.01%), PEG-SOD (PSOD, 50U/ml) or the SOD inhibitor (ammonium tetrathiomolybdate, 4 μM) [38] before an assay. Fluorescence (Ex 540 nm/Em 575 nm) was measured in an O_2 -regulated plate reader (CLARIOstar, BMG Labtech).

2.10. Statistics

Data denote the mean \pm S.E.M. of at least 3–5 different bEnd.3 cell cultures and were processed using Graphpad Prism 8, with some preliminary handling steps performed using MARS data analysis software (BMG Labtech). Significance was assessed using either a paired Student's *t*-test or one- or two-way ANOVA followed by a Bonferroni Post Hoc test where appropriate, with significance confirmed by $P < 0.05$.

3. Results

3.1. Sulforaphane induces Nrf2 nuclear translocation and antioxidant enzymes in bEnd.3 cells

Treatment of bEnd.3 cells under 18 kPa O_2 with the Nrf2 inducer sulforaphane (SFN, 2.5 μM) increased nuclear accumulation of Nrf2 over 1–2 h (Fig. 1A). Nrf2 gene silencing had negligible effects on basal HO-1

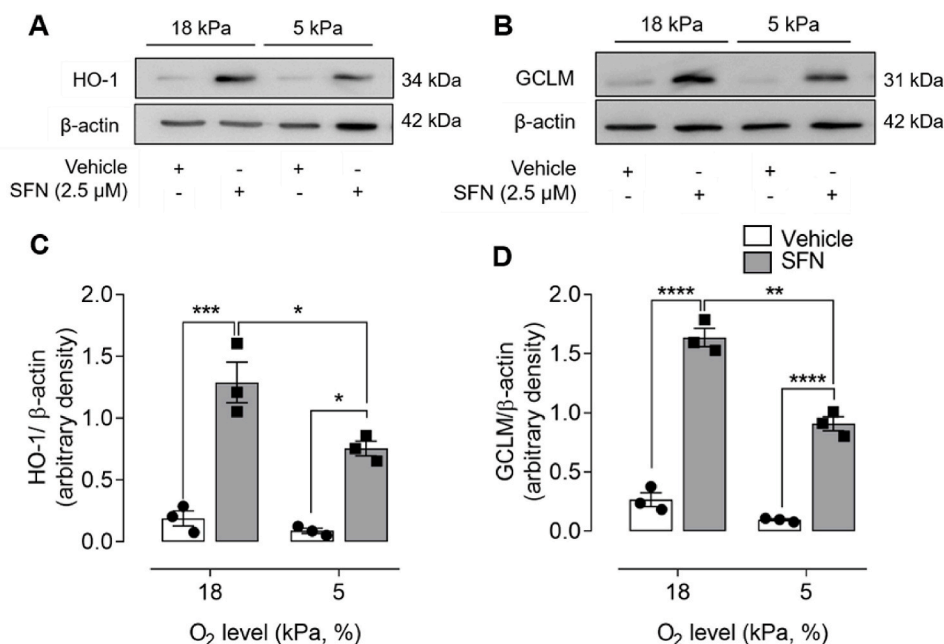


Fig. 3. Adaptation to physiological normoxia diminishes sulforaphane induced HO-1 and GCLM protein expression

bEnd.3 cells were cultured under either 18 or 5 kPa O₂ for 5 d and then treated with vehicle (0.01% DMSO) or sulforaphane (SFN, 2.5 μM) for 24 h. Cell lysates were immunoblotted for HO-1 (A) and GCLM (B) expression relative to β-actin and analysed by densitometry (C–D). Data denote mean ± S.E.M., n = 3 independent bEnd.3 cultures, two-way ANOVA, *P < 0.05. **P < 0.01, ***P < 0.001, ****P < 0.0001.

protein levels but abrogated SFN-induced upregulation of HO-1 (Fig. 1B and C) and NQO1 (data not shown) expression. In initial experiments, we established that physiological concentrations of SFN (0.5–2.5 μM) [14] significantly upregulated Nrf2 mediated HO-1 protein levels (12–24 h, Supplementary Fig. S1A) and mRNA expression of HO-1, NQO1, Bach1 and Keap1 (4 h, Supplementary Fig. S1B).

3.2. Real-time measurement of intracellular O₂ level in bEnd.3 cells

We and others have emphasized the importance of monitoring O₂ gradients between culture medium and cell cytosol [20,22,39,40], and here report the first real-time measurement of intracellular O₂ in brain microvascular endothelial cells (bEnd.3) using the cell-penetrating phosphorescent nanoparticle probe MitoXpress®-INTRA [26]. Phosphorescence lifetime in bEnd.3 cells and medium was measured during stepwise reductions of O₂ (18 kPa–0 kPa) within an O₂-regulated, time-resolved fluorescence plate reader (Fig. 2A). The relationship between ambient O₂ levels in the plate reader and phosphorescence lifetime is illustrated in Fig. 2B. An intracellular O₂ level of 3.4 ± 0.1 kPa (inset, Fig. 2B) was measured in cells cultured under 5 kPa O₂, recapitulating levels in the cortex of awake mice [41], with dissolved O₂ in the medium (5.2 ± 0.2 kPa) similar to the O₂ level (5 kPa) in the plate reader.

3.3. Adaptation of bEnd.3 cells to 5 kPa O₂ does not induce a hypoxic phenotype

To determine whether adaptation of bEnd.3 cells under 5 kPa O₂ induces hypoxic responses, we examined stabilization of HIF-1α, a key modulator of transcriptional responses to hypoxia. In the presence of oxygen, HIF-1α is degraded via prolyl hydroxylation [42], involving HIF-1α association with von Hippel-Lindau protein E3 ubiquitin ligase complex to promote degradation [42,43]. As intracellular O₂ availability decreases, these enzymes are no longer able to hydroxylate HIF-1α subunits, resulting in stabilization and upregulation of HIF-1α protein levels. When bEnd.3 cells were adapted to 18, 5 or 1 kPa O₂, HIF-1α stabilization was only detected under hypoxia (Fig. 2C), confirming the absence of a hypoxic phenotype in cells maintained long-term under physiological normoxia (5 kPa O₂).

3.4. Effects of ambient O₂ levels on cell viability, ATP and GSH content and proliferation

Adaptation of bEnd.3 cells to 5 kPa O₂ had no effect on cell viability, as evidenced by negligible changes in mitochondrial dehydrogenase activity (data not shown) or intracellular ATP levels (5 kPa O₂: 24.3 ± 2.2 vs 18 kPa O₂: 20.7 ± 1.7 nmol/mg.protein) (Fig. 2D). Intracellular GSH (Fig. 2E) and catalase (Fig. 2F) levels were significantly lower in bEnd.3 cells adapted to 5 kPa O₂, consistent with our previous findings in airway epithelial cells [23] and other studies in epidermoid carcinoma cells [40]. Total intracellular GSH levels were similar in bEnd.3 cells in passages 7–15 (data not shown). Moreover, bEnd.3 cell proliferation was decreased under 5 kPa O₂ compared to 18 kPa O₂ (Fig. 2G). The implications of these findings are that the enhanced oxidative stress during standard cell culture under hyperoxia (18 kPa O₂) is attenuated in cells adapted to physiological normoxia (5 kPa O₂).

3.5. Physiological normoxia attenuates sulforaphane induced Nrf2 regulated enzyme expression

To determine whether Nrf2 redox signaling was affected by changes in ambient O₂ levels, bEnd.3 cells were adapted to 18 or 5 kPa O₂ and Nrf2 induced antioxidant enzyme expression determined by immunoblotting. Although basal levels of HO-1 and GCLM expression were affected negligibly following adaptation to physiological normoxia (5 kPa O₂), upregulation of Nrf2 regulated enzyme expression by SFN (2.5 μM, 24 h) was significantly attenuated in cells adapted to 5 kPa O₂ (Fig. 3). These findings are consistent with reports of diminished induction of antioxidant enzymes by Nrf2 in HUVEC [22], airway epithelial cells [23], RAW264.7 macrophages [44] and epidermoid carcinoma cells [40] under physiological normoxia.

3.6. Reoxygenation induced superoxide production in bEnd.3 cells under 18 kPa O₂

bEnd.3 cells adapted to 18 kPa O₂ were incubated with the chemiluminescent probe L-012 to investigate reactive oxygen species generation during hypoxia-reoxygenation. As shown in Fig. 4A, reoxygenation induced free radical generation was significantly inhibited by SOD (100U/ml) and PEG-SOD (PSOD, 50U/ml), whereas PEG-

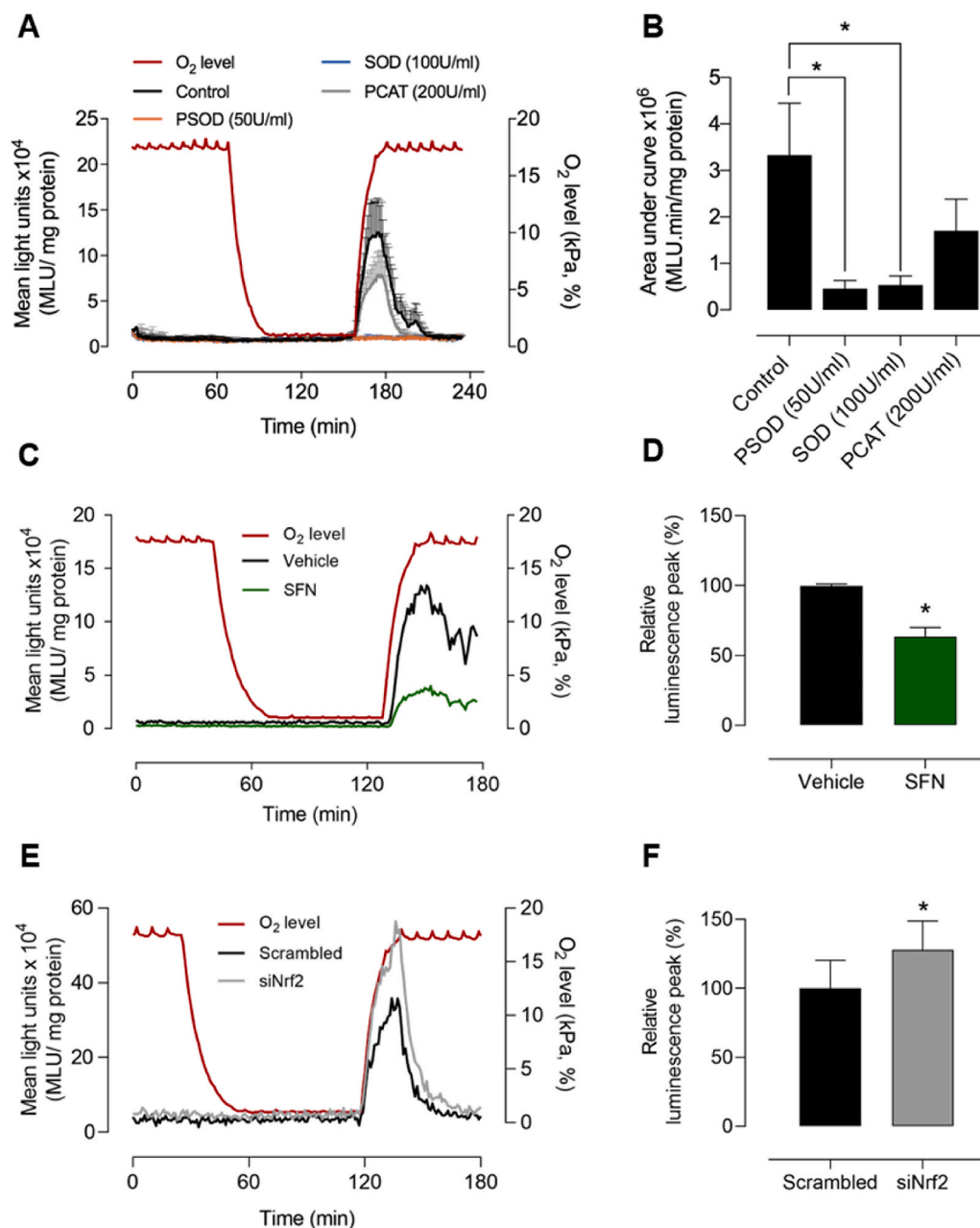


Fig. 4. Sulforaphane reduces and Nrf2 gene silencing enhances reoxygenation induced superoxide production in bEnd.3 cells under 18 kPa O₂

bEnd.3 cells were cultured under 18 kPa O₂ for 5 d. (A) Cells were treated with vehicle (0.01% DMSO), PEG-superoxide dismutase (PSOD, 50U/ml), superoxide dismutase (SOD, 100U/ml) or PEG-catalase (PCAT, 200U/ml) for 30 min prior to incubation with L-012 (see Methods). Cells were rapidly transferred to an O₂-regulated plate reader and subjected to hypoxia (1 h) and reoxygenation under 18 kPa O₂, with L-012 luminescence measured in the absence (control) or presence of inhibitors. O₂ levels inside the plate reader are indicated by the red line (right axis) and mean light units (MLU/mg protein) on the left axis. (B) Area under L-012 traces during reoxygenation (160–190 min) for each treatment. (C) Representative L-012 traces in cells pre-treated with vehicle (0.01% DMSO) or SFN (2.5 μ M, 24 h) and (D) relative peak luminescence (120–140 min, % vehicle) on reoxygenation. (E) Representative L-012 traces in cells transfected with scrambled or Nrf2 siRNA and (F) relative peak luminescence (125–140 min, % scrambled siRNA). Data denote mean \pm S.E. M., n = 3–4 independent bEnd.3 cultures, one-way ANOVA, *P < 0.05.

CAT (PCAT, 200U/ml) led to a non-significant decrease in L-012 luminescence, suggesting that reoxygenation most likely increases superoxide generation. Fig. 4B summarizes the changes in luminescence induced by reoxygenation in the absence and presence of scavengers of reactive oxygen species.

As NADP(H) oxidases (NOX) have been implicated as a source of free radical generation in cerebral ischemia-reperfusion [45,46], bEnd.3 cells adapted to 18 kPa O₂ were pre-treated with the NOX inhibitor VAS2870 (5 μ M) for 30 min, incubated with L-012 and then exposed to hypoxia (1 kPa O₂, 1 h) and reoxygenation. As shown in Supplementary Fig. S2, reoxygenation induced increases in L-012 luminescence were unaffected by VAS2870, suggesting that NADPH oxidases are an unlikely source of acute reoxygenation induced free radical generation in bEnd.3 cells.

3.7. Sulforaphane pretreatment protects against reoxygenation induced superoxide generation

To determine whether upregulation of Nrf2 target genes attenuates reoxygenation induced free radical generation, bEnd.3 cells were adapted to 18 kPa O₂ and pre-treated with either vehicle (DMSO 0.01%) or SFN (2.5 μ M) for 24 h. SFN significantly diminished reoxygenation induced L-012 luminescence (Fig. 4C and D) and moreover, in cells transfected with scrambled or Nrf2 siRNA, we confirmed that silencing Nrf2 significantly enhances the L-012 luminescence signal during reoxygenation (Fig. 4E and F).

3.8. Reoxygenation induced free radical generation is diminished in bEnd.3 cells under 5 kPa O₂

Basal and reoxygenation induced L-012 luminescence was significantly lower in bEnd.3 cells adapted to 5 kPa O₂ (Fig. 5A) compared to 18 kPa O₂ (Fig. 4A). Although reoxygenation induced changes in L-012

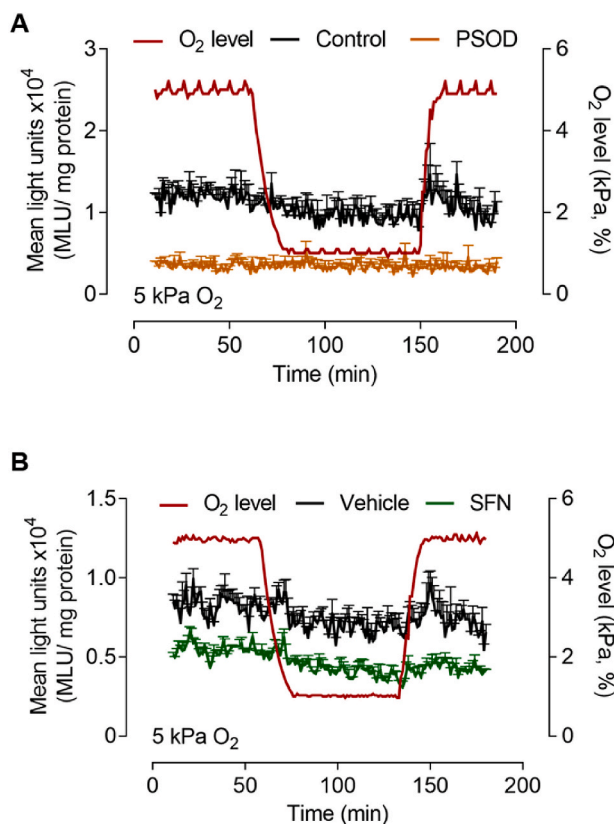


Fig. 5. Adaptation to 5 kPa O₂ diminishes reoxygenation induced reactive oxygen species generation in bEnd.3 cells

bEnd.3 cells were cultured under 5 kPa O₂ for 5 d. (A) Cells were treated with vehicle (0.01% DMSO, black line, control) or PEG-superoxide dismutase (PSOD, 50 U/ml, orange line) for 30 min prior to incubation with L-012. Cells were transferred to an O₂-regulated plate reader and subjected to hypoxia (1 h) and reoxygenation under 5 kPa O₂. O₂ levels inside the plate reader are indicated by the red line (right axis) and mean light units (MLU/mg protein) on the left axis. (B) bEnd.3 cells pre-treated with vehicle (0.01% DMSO) or SFN (2.5 μM, 24 h) prior to hypoxia (1 h) and reoxygenation under 5 kPa O₂. Data denote mean ± S.E.M, n = 3 independent bEnd.3 cultures. (For interpretation of the references to color in this figure legend, the reader is referred to the Web version of this article.)

luminescence were not significant, the signal appeared decreased in the presence of PSOD (Fig. 5A) or following pretreatment of cells with SFN (2.5 μM, 24 h) (Fig. 5A and B). This attenuated intracellular free radical production in bEnd.3 cells under 5 kPa O₂ is consistent with previous studies in RAW264.7 macrophages [44], epidermoid carcinoma cells [40], SH-SY5Y neuronal cells [47] and skeletal myoblasts/myotubes [48].

3.9. Reoxygenation-induced increases in MitoSOX red fluorescence

To further validate reoxygenation mediated changes in L-012 luminescence, we examined mitochondrial reactive oxygen species generation in bEnd.3 cells adapted to 18 or 5 kPa O₂. Hypoxia-reoxygenation increased MitoSOX fluorescence in cells under 18 kPa O₂ with negligible changes detectable under 5 kPa O₂ (Fig. 6A and B). As shown in Supplementary Fig. S3, reoxygenation induced increases in MitoSOX fluorescence were unaffected by inhibition of complex I (rotenone, 1 μM) or eNOS (L-NAME, 100 μM). Notably, pretreatment of cells with SFN (2.5 μM, 12 h) significantly attenuated reoxygenation induced MitoSOX fluorescence in cells under 18 but not 5 kPa O₂ (Fig. 6C–E), consistent with the negligible changes in L-012 luminescence observed in bEnd.3 cells during acute reoxygenation under 5 kPa. To exclude the possibility

that changes in ambient O₂ levels affected MitoSOX fluorescence, the probe was dissolved in 1% FCS medium and a 96-well plate transferred to the plate reader under 18 or 5 kPa O₂. When H₂O₂ (10 μM) was injected using on-board injector units in the plate reader, MitoSOX fluorescence was similar under 18 and 5 kPa O₂ (data not shown).

3.10. Reoxygenation-induced increases in FeRhoNox fluorescence

Based on caveats associated with the specificity of L-012 and MitoSOX Red, such as non-specific oxidation of the probes [49,50], further indirect measurements of reoxygenation induced superoxide production were conducted using an Fe²⁺-specific fluorescent indicator, FeRhoNoxTM-1, in bEnd.3 adapted to 18 or 5 kPa O₂. Inhibition of superoxide dismutase by ammonium tetrathiomolybdate has been reported to prolong the cytosolic Fe²⁺ signal in dermal fibroblasts and endothelial cells challenged with UVA radiation [37]. As shown in Fig. 7A, increases in FeRhoNox-1 fluorescence during reoxygenation under 18 kPa O₂ were inhibited by PEG-SOD and potentiated by inhibition of SOD with ammonium tetrathiomolybdate. Previous studies have shown that mitochondria exposed to superoxide release iron from iron-sulphur clusters, indicating that increased radical production will lead to an increase in free iron [51,52]. In the present study, we exploited the fact that increases in free iron would increase FeRhoNoxTM-1 fluorescence, and thus changes in fluorescence served as an indirect measure of superoxide generation in bEnd.3 cells subjected to reoxygenation. Notably, reoxygenation induced FeRhoNox-1 fluorescence was attenuated in bEnd.3 cells adapted to 5 kPa O₂ (Fig. 7B). Together with our findings of reoxygenation induced changes in L-012 luminescence and MitoSOX fluorescence, FeRhoNox-1 measurements suggest that superoxide is the most likely free radical generated during acute reoxygenation induced oxidative stress in bEnd.3 cells.

4. Discussion

Changes in ambient O₂ levels during cell culture *in vitro* alter (i) ion channel and kinase activities [53–55], (ii) endothelial Ca²⁺ signaling, nitric oxide bioavailability and their sensitivity to Ca²⁺ overload [24, 25], and (iii) induction of Nrf2-targeted antioxidant defenses [22,23, 56]. We here further demonstrate that the redox phenotype of mouse brain microvascular endothelial cells is critically affected by ambient oxygen levels. Endothelial cells lining the blood-brain barrier *in vivo* are exposed to O₂ levels ranging between ~3 and 7 kPa, yet the majority of studies in brain endothelial and other cell types *in vitro* have employed standard culture conditions in which cells are exposed to hyperoxia (18 kPa O₂) and therefore sustained oxidative stress [20].

Using the O₂-sensitive nanoparticle probe MitoXpress[®]-INTRA, we obtained the first measurements of intracellular O₂ (3.4 kPa) in bEnd.3 endothelial cells, recapitulating O₂ levels measured in brain endothelium *in vivo*. Importantly, long-term adaptation of bEnd.3 cells to 5 kPa O₂ was not associated with HIF-1α stabilization, confirming the absence of a hypoxic phenotype under physiological normoxia. Moreover, as gradients exist between ambient O₂ levels in a Scitive workstation, medium and cytosol, it is critical that medium and intracellular O₂ levels are measured simultaneously [20,22]. MitoXpress[®]-INTRA has been used to measure intracellular O₂ in umbilical vein endothelial cells [22, 24], mouse embryonic fibroblasts [26], cortical neurons [57] and now in brain microvascular endothelial cells.

Adaptation of bEnd.3 cells under 5 kPa O₂ did not affect cell viability or intracellular ATP levels, but significantly decreased levels of intracellular GSH and catalase, suggesting that cells under physiological normoxia experience less oxidative stress [20,58]. Basal expression of Nrf2-regulated antioxidant enzymes was similar in bEnd.3 cells cultured under 18 or 5 kPa O₂, however SFN mediated induction of HO-1 and GCLM was significantly attenuated in cells adapted to 5 kPa O₂. Our finding of diminished HO-1 induction is in agreement with our previous studies in human umbilical vein and coronary artery endothelial cells

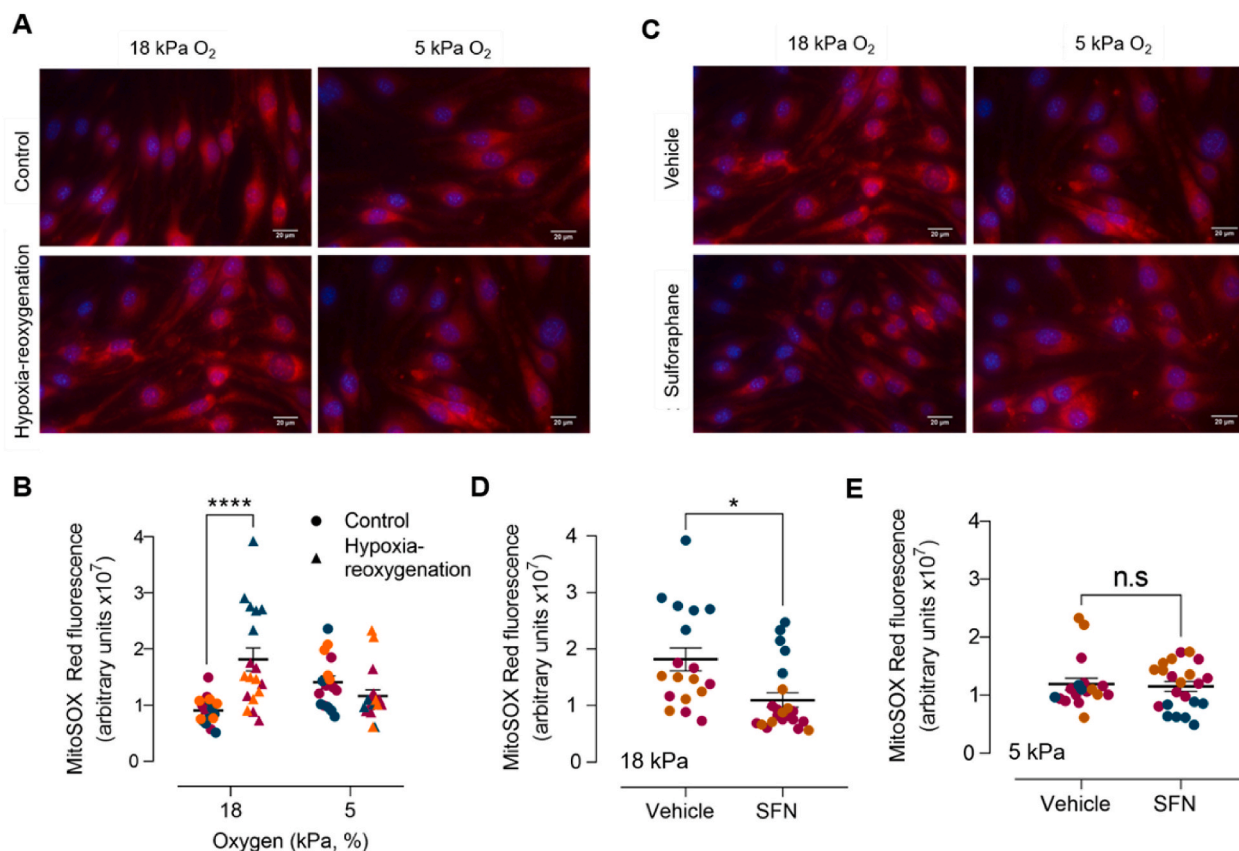


Fig. 6. Effects of sulforaphane pretreatment on reoxygenation induced mitochondrial reactive oxygen species generation in bEnd.3 cells adapted to 18 kPa or 5 kPa O₂

bEnd.3 cells seeded in Ibidi μ -Slide 8-well chambers were cultured under 18 or 5 kPa O₂ for 5 d. Cells were subjected to hypoxia (1 kPa O₂, 1 h) and loaded with MitoSOXTM Red for 5 min before the start of 30 min reoxygenation under 18 or 5 kPa O₂, respectively. Control cells were loaded with MitoSOXTM Red during the last 30 min of an experiment. Cells were fixed with 4% paraformaldehyde and images acquired using a Nikon Diaphot microscope with a 40 \times objective. (A) Representative images of MitoSOX fluorescence and DAPI stained nuclei after 30 min reoxygenation and (B) quantification of MitoSOX fluorescence. (C) bEnd.3 cells were pre-treated with vehicle (0.01% DMSO) or SFN (2.5 μ M) for 24 h before exposure to hypoxia (1 h) and reoxygenation under 18 or 5 kPa O₂, respectively. Representative images of MitoSOX fluorescence and DAPI stained nuclei after 30 min reoxygenation and (D–E) quantitation of MitoSOX fluorescence. Each symbol in panels B, D and E represents the mean fluorescence from at least 10 cells in a field of view, with each color denoting a different bEnd.3 experiment with at least 6 different fields of view. Data denote mean \pm S.E.M., n = 18–20 fields of view in each of 3 independent bEnd.3 cell cultures, two-way ANOVA followed by Bonferroni post-hoc analysis, ****P < 0.0001. Scale bar = 20 μ m. (For interpretation of the references to color in this figure legend, the reader is referred to the Web version of this article.)

[22] and other studies in lung epithelial cells [23] and human dental pulp stem cells [56] cultured under relevant physiological O₂ levels. Notably, electrophile and nitric oxide mediated induction of HO-1 in human endothelial cells adapted 5 kPa O₂ is attenuated, but reversible on re-exposure of cells to 18 kPa O₂ or following silencing of the Nrf2 repressor Bach1 [22].

Our previous studies of reperfusion injury in a rodent model of transient ischemic stroke established that activation of Nrf2 antioxidant defenses by SFN affords neurovascular and neurological protection [17, 18]. To mimic ischemia-reperfusion injury in stroke at a cellular level, bEnd.3 cells were adapted to either 18 or 5 kPa O₂ and subjected to hypoxia (1 kPa O₂) and reoxygenation under 18 or 5 kPa O₂, respectively. Reoxygenation-induced increases in L-012 luminescence in cells adapted to 18 kPa O₂ was abrogated by SOD and polyethylene glycol SOD, implicating superoxide as the most likely free radical species generated during reoxygenation. Although polyethylene glycol catalase led to a non-significant decrease in reoxygenation-induced free radical production, we cannot exclude that inhibition of L-012 luminescence signal by SOD or polyethylene glycol SOD may be due to generation of superoxide from molecular oxygen during L-012 oxidation by H₂O₂/peroxidase [59]. We further demonstrated that upregulation of Nrf2-regulated antioxidant enzymes by SFN led to a significant decrease

in reoxygenation induced free radicals (Fig. 4C and D), whilst silencing Nrf2 transcriptional activity enhanced reoxygenation induced free radical generation (Fig. 4E and F).

Reoxygenation induced changes in L-012 luminescence were lower in bEnd.3 cells adapted to 5 kPa O₂ (Fig. 5), although L-012 signals trended to decrease in the presence of PEG-SOD or following SFN pretreatment. In this context, studies in macrophages [44], epidermoid carcinoma cells [40] and dental pulp stem cells [60], as well as, our experiments in human endothelial cells (data not shown) confirm that oxidative stress is lower in cells adapted to physiological normoxia. Thus, under standard, hyperoxic cell culture conditions, the redox phenotype of cells is characterized by an upregulation of Nrf2-regulated gene transcription to counteract enhanced reactive oxygen species generation and sustained oxidative stress [20].

We further investigated the redox status of bEnd.3 cells exposed to hypoxia-reoxygenation by assaying MitoSOX fluorescence as an index of mitochondrial reactive oxygen species generation. Reoxygenation significantly increased MitoSOX fluorescence in bEnd.3 cells adapted to 18 but not 5 kPa O₂, and notably SFN pretreatment only attenuated reoxygenation-induced MitoSOX fluorescence in cells adapted to 18 kPa O₂, further supporting our finding that SFN inhibits acute reoxygenation induced increases in L-012 luminescence. Reoxygenation induced

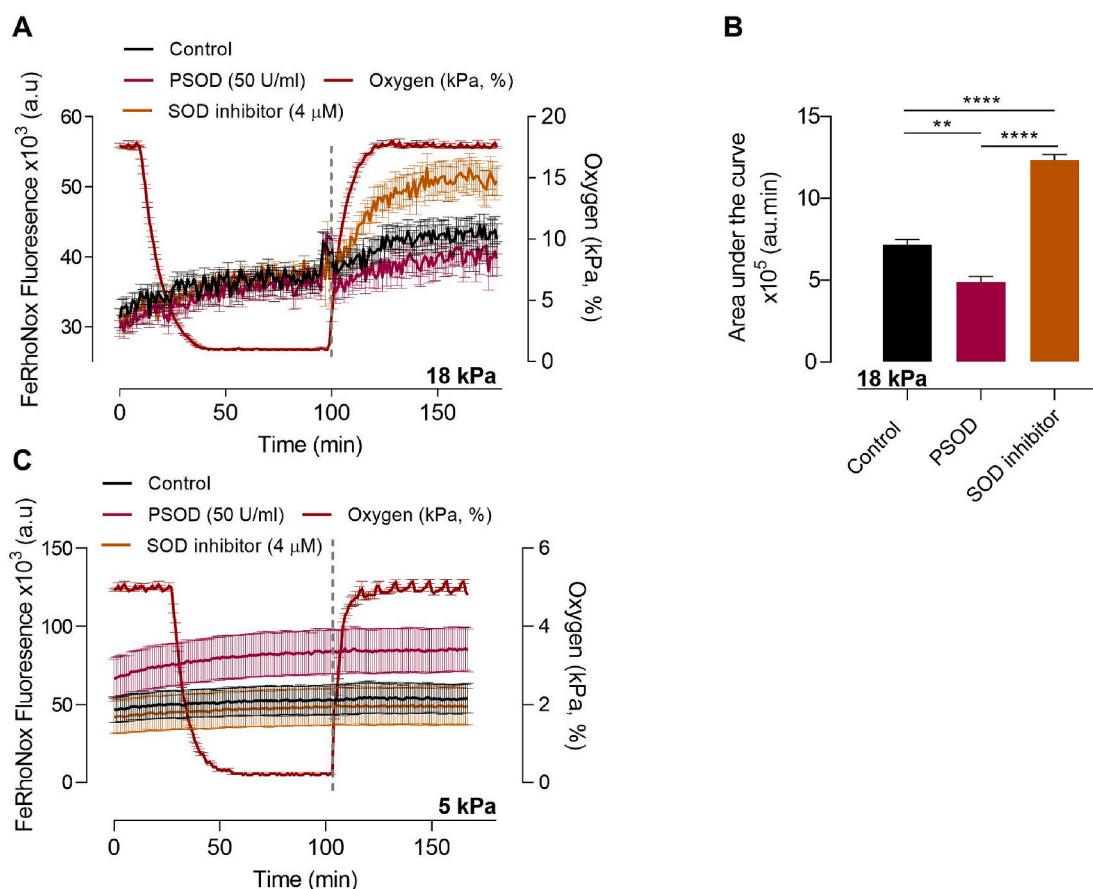


Fig. 7. Reoxygenation induces intracellular Fe^{2+} release in bEnd.3 cells adapted to 18 kPa O_2 but not 5 kPa O_2 .

bEnd.3 cells were cultured under 18 or 5 kPa O_2 for 5 d. Cells were then incubated with the Fe^{2+} -selective probe FeRhoNoxTM-1 (5 μ M, 1 h) in HBSS in the presence of vehicle (0.01% DMSO, control, black line), PEG-superoxide dismutase (PSOD, 50U/ml, pink line) or a SOD inhibitor (4 μ M ammonium tetrathiomolybdate, orange line). (A-B) Mean FeRhoNox fluorescence traces in cells exposed to hyperoxia (18 kPa O_2), hypoxia (1 kPa O_2 , 1 h) and reoxygenation under 18 kPa O_2 and area under the curve following reoxygenation (dashed line indicates reoxygenation period 100–160 min) for each treatment. (C) Mean FeRhoNox fluorescence traces in cells adapted to physiological normoxia (5 kPa O_2), hypoxia (1 kPa O_2 , 1 h) and reoxygenation under 5 kPa O_2 . Data denote mean \pm S.E.M from 3 to 4 independent bEnd.3 cell cultures, one-way ANOVA followed by Bonferroni post-hoc analysis, ** $P < 0.001$, **** $P < 0.0001$. (For interpretation of the references to color in this figure legend, the reader is referred to the Web version of this article.)

increases MitoSOX fluorescence were unaffected by L-NAME or a pan-NADPH oxidase inhibitor (VAS2870), suggesting that free radical generation in bEnd.3 cells was unlikely due to eNOS or NOX. Although VAS2870 had no effect on cell viability or reoxygenation induced free radical generation, we cannot exclude that VAS2870 and other NOX inhibitors may have off-target effects via thiol alkylation, inhibition of mitochondrial respiration and cytotoxicity [61]. Furthermore, although undetectable in our study, we cannot exclude the possibility of enhanced reactive oxygen species generation during hypoxia, as it has recently been suggested that acute hypoxia drives the import of Na^+ into the mitochondrial matrix, reducing inner mitochondrial fluidity and consequently concentrating the production of superoxide at complex III [62].

To further characterize reoxygenation-induced free radical generation in bEnd.3 cells, release of intracellular Fe^{2+} was monitored as an indirect measure of intracellular superoxide generation. By using PEG-SOD and a SOD inhibitor, we demonstrated for the first time that changes in FeRhoNox-1 fluorescence provide a useful measure of reoxygenation-induced superoxide generation in brain microvascular endothelial cells. Release of labile iron is closely associated with reactive oxygen species generation, and iron accumulation occurs in stroke [63], traumatic brain injury [64] and neurodegenerative disorders [65,66]. Furthermore, mitochondria exposed to superoxide anions release iron from iron-sulphur clusters, such that increased free radical generation

will result in increased free iron [51,52]. Increases in superoxide in the presence of SOD inhibition reduces Fe^{3+} in the ferritin core to Fe^{2+} , releasing Fe^{2+} into the cytoplasm [37,67].

Our study establishes that bEnd.3 cells adapted to long-term to hyperoxia (18 kPa O_2) exhibit heightened sensitivity to hypoxia-reoxygenation, resulting in increased reactive oxygen species generation on reoxygenation. Studies *in vivo* have reported that following ischemia-reperfusion injury in the heart and brain, accumulation of succinate in mitochondria drives reactive oxygen species generation via reverse electron transport at mitochondrial complex I, and that oxidative damage can be decreased by reducing succinate accumulation [68]. In the present study, activation of Nrf2 by SFN significantly diminished reoxygenation induced free radical generation while silencing of Nrf2 exacerbated free radical generation, implicating Nrf2 in protection against reoxygenation/reperfusion injury. In this context, Nrf2 has been shown to significantly affect the mitochondrial membrane potential, fatty acid oxidation and the availability of substrates including succinate [69,70]. As Nrf2 deficient cells and mice *in vivo* are more sensitive to oxidative damage [71,72], activation of Nrf2 by SFN not only upregulates antioxidant defense enzymes but importantly also influences mitochondrial substrate utilization and respiration [69,70].

As generation of reactive oxygen species was attenuated in bEnd.3 cells adapted to physiological normoxia, it is possible that the probes L-012 and MitoSOX Red used in this study and other studies lack sufficient

sensitivity to monitor low levels of radical generation in response to acute reoxygenation. Although recent advances in multiphoton redox and pO₂ imaging have enabled elegant quantification of metabolic processes under different ambient O₂ levels [73], we consider it important to ensure that decreasing ambient oxygen levels from 18 kPa O₂ does not result in HIF-1 α stabilization and activation hypoxic signaling pathways. In this context, we previously reported that long-term (~5 d) culture of vascular cells under physiological O₂ levels is required to exclude a hypoxic phenotype [22,24].

In view of the caveats concerning luminescence and fluorescence indicators [49,50], further studies are warranted using novel genetic biosensors for high-resolution, real-time imaging of reactive oxygen and nitrogen species in single cells and subcellular compartments [74,75]. Conducting such experiments in cells adapted long-term under controlled and physiologically relevant O₂ levels will prove challenging, but we are convinced that such *in vitro* cell culture models, in particular targeting biosensors to mitochondria in live cells, will provide insights for the design of novel therapeutics for treatment cerebral, coronary, renal and hepatic ischemia-perfusion injury.

Author contributions

G.W., P.A.F. and G.E.M. conceptualized the study; G.W. developed the methodology, T.P.K. assisted with MitoXpress®-Intra experiments and R.C.M.S. with FeRhoNox-1 experiments; G.W., S.S. and M.J.S. performed the experiments; G.W. and G.E.M. wrote the manuscript which was reviewed by all authors. G.E.M. is the guarantor of this study, with responsibility for the integrity of the data and accuracy of the data analysis.

Declaration of competing interest

The authors declare no competing interests.

Acknowledgements

Supported by British Heart Foundation (FS/16/67/32548, G.E.M.), Heart Research UK (RG2673, G.E.M.), and EVGEN R&D Grant (G.E.M.). We gratefully acknowledge Dr David Begley (King's College London) for supply of bEnd.3 endothelial cells for initial experiments and Prof. T. Kavanagh (University of Washington, WA, USA) for the GCLM antibody. We thank Dr Ron Jacob (King's College London) and Dr Sarah J. Chapple (King's College London) for their helpful discussions.

Appendix A. Supplementary data

Supplementary data to this article can be found online at <https://doi.org/10.1016/j.redox.2020.101708>.

References

- M.S. Phipps, C.A. Cronin, Management of acute ischemic stroke, *BMJ* 368 (2020) 16983.
- B.C.V. Campbell, D.A. De Silva, M.R. Macleod, S.B. Coutts, L.H. Schwamm, S. M. Davis, G.A. Donnan, Ischaemic stroke, *Nat Rev Dis Primers* 5 (2019) 70.
- M. Endres, U. Dirnagl, Ischemia and stroke, *Adv. Exp. Med. Biol.* 513 (2002) 455–473.
- U. Dirnagl, C. Iadecola, M.A. Moskowitz, Pathobiology of ischaemic stroke: an integrated view, *Trends Neurosci.* 22 (1999) 391–397.
- O. Peters, T. Back, U. Lindauer, C. Busch, D. Megow, J. Dreier, U. Dirnagl, Increased formation of reactive oxygen species after permanent and reversible middle cerebral artery occlusion in the rat, *J. Cerebr. Blood Flow Metabol.* 18 (1998) 196–205.
- J.L. Yang, S. Mukda, S.D. Chen, Diverse roles of mitochondria in ischemic stroke, *Redox Biol* 16 (2018) 263–275.
- W. Hacke, M. Kaste, E. Bluhmki, M. Brozman, A. Davalos, D. Guidetti, V. Larrue, K. R. Lees, Z. Medeghri, T. Machnig, D. Schneider, R. von Kummer, N. Wahlgren, D. Toni, E. Investigators, Thrombolysis with alteplase 3 to 4.5 hours after acute ischemic stroke, *N. Engl. J. Med.* 359 (2008) 1317–1329.
- J. Emberson, K.R. Lees, P. Lyden, L. Blackwell, G. Albers, E. Bluhmki, T. Brott, G. Cohen, S. Davis, G. Donnan, J. Grotta, G. Howard, M. Kaste, M. Koga, R. von Kummer, M. Lansberg, R.I. Lindley, G. Murray, J.M. Olivrot, M. Parsons, B. Tilley, D. Toni, K. Toyoda, N. Wahlgren, J. Wardlaw, W. Whiteley, G.J. del Zoppo, C. Baigent, P. Sandercock, W. Hacke, G. Stroke Thrombolysis Trialists' Collaborative, Effect of treatment delay, age, and stroke severity on the effects of intravenous thrombolysis with alteplase for acute ischaemic stroke: a meta-analysis of individual patient data from randomised trials, *Lancet* 384 (2014) 1929–1935.
- N.J. Spratt, G.A. Donnan, D.D. McLeod, D.W. Howells, Salvaged stroke ischaemic penumbra shows significant injury: studies with the hypoxia tracer FMISO, *J. Cerebr. Blood Flow Metabol.* 31 (2011) 934–943.
- P.A. Fraser, The role of free radical generation in increasing cerebrovascular permeability, *Free Radical Biol. Med.* 51 (2011) 967–977.
- M.D. Sweeney, Z. Zhao, A. Montagne, A.R. Nelson, B.V. Zlokovic, Blood-brain barrier: from physiology to disease and back, *Physiol. Rev.* 99 (2019) 21–78.
- C.L. Allen, U. Bayraktutan, Oxidative stress and its role in the pathogenesis of ischaemic stroke, *Int. J. Stroke* 4 (2009) 461–470.
- N.J. Abbott, L. Ronnback, E. Hansson, Astrocyte-endothelial interactions at the blood-brain barrier, *Nat. Rev. Neurosci.* 7 (2006) 41–53.
- A.T. Dinkova-Kostova, R.V. Kostov, Glucosinolates and isothiocyanates in health and disease, *Trends Mol. Med.* 18 (2012) 337–347.
- T. Suzuki, M. Yamamoto, Molecular basis of the Keap1-Nrf2 system, *Free Radical Biol. Med.* 88 (2015) 93–100.
- T. Ishii, K. Itoh, E. Ruiz, D.S. Leake, H. Unoki, M. Yamamoto, G.E. Mann, Role of Nrf2 in the regulation of CD36 and stress protein expression in murine macrophages: activation by oxidatively modified LDL and 4-hydroxynonenal, *Circ. Res.* 94 (2004) 609–616.
- A. Alfieri, S. Srivastava, R.C. Siow, D. Cash, M. Mado, M.R. Duchon, P.A. Fraser, S. C. Williams, G.E. Mann, Sulforaphane preconditioning of the Nrf2/HO-1 defense pathway protects the cerebral vasculature against blood-brain barrier disruption and neurological deficits in stroke, *Free Radical Biol. Med.* 65 (2013) 1012–1022.
- S. Srivastava, A. Alfieri, R.C. Siow, G.E. Mann, P.A. Fraser, Temporal and spatial distribution of Nrf2 in rat brain following stroke: quantification of nuclear to cytoplasmic Nrf2 content using a novel immunohistochemical technique, *J. Physiol.* 591 (2013) 3525–3538.
- A. Jazwa, A.I. Rojo, N.G. Innamorato, M. Hesse, J. Fernandez-Ruiz, A. Cuadrado, Pharmacological targeting of the transcription factor Nrf2 at the basal ganglia provides disease modifying therapy for experimental parkinsonism, *Antioxidants Redox Signal.* 14 (2011) 2347–2360.
- T.P. Keeley, G.E. Mann, Defining physiological normoxia for improved translation of cell physiology to animal models and humans, *Physiol. Rev.* 99 (2019) 161–234.
- S. Parrinello, E. Samper, A. Krtoic, J. Goldstein, S. Melov, J. Campisi, Oxygen sensitivity severely limits the replicative lifespan of murine fibroblasts, *Nat. Cell Biol.* 5 (2003) 741–747.
- S.J. Chapple, T.P. Keeley, D. Mastronicola, M. Arno, G. Vizcay-Barrena, R. Fleck, R. C. Siow, G.E. Mann, Bach1 differentially regulates distinct Nrf2-dependent genes in human venous and coronary artery endothelial cells adapted to physiological oxygen levels, *Free Radical Biol. Med.* 92 (2016) 152–162.
- A. Kumar, L.A. Dailey, M. Swedrowska, R. Siow, G.E. Mann, G. Vizcay-Barrena, M. Arno, I.S. Mudway, B. Forbes, Quantifying the magnitude of the oxygen artefact inherent in culturing airway cells under atmospheric oxygen versus physiological levels, *FEBS Lett.* 590 (2016) 258–269.
- T.P. Keeley, R.C.M. Siow, R. Jacob, G.E. Mann, A PP2A-mediated feedback mechanism controls Ca²⁺-dependent NO synthesis under physiological oxygen, *Faseb. J.* 31 (2017) 5172–5183.
- T.P. Keeley, R.C.M. Siow, R. Jacob, G.E. Mann, Reduced SERCA activity underlies dysregulation of Ca(2+) homeostasis under atmospheric O₂ levels, *Faseb. J.* 32 (2018) 2531–2538.
- A. Fercher, S.M. Borisov, A.V. Zhdanov, I. Klimant, D.B. Papkovsky, Intracellular O₂ sensing probe based on cell-penetrating phosphorescent nanoparticles, *ACS Nano* 5 (2011) 5499–5508.
- K.K. Sharman, A. Periasamy, H. Ashworth, J.N. Demas, Error analysis of the rapid lifetime determination method for double-exponential decays and new windowing schemes, *Anal. Chem.* 71 (1999) 947–952.
- X. Cheng, S.J. Chapple, B. Patel, W. Puszyk, D. Sugden, X. Yin, M. Mayr, R.C. Siow, G.E. Mann, Gestational diabetes mellitus impairs Nrf2-mediated adaptive antioxidant defenses and redox signaling in fetal endothelial cells in utero, *Diabetes* 62 (2013) 4088–4097.
- S. Srivastava, P.J. Blower, A.A. Auldool, R.C. Hider, G.E. Mann, R.C. Siow, Cardioprotective effects of Cu(II)ATSM in human vascular smooth muscle cells and cardiomyocytes mediated by Nrf2 and DJ-1, *Sci. Rep.* 6 (2016) 7.
- P.J. Hissin, R. Hilf, A fluorometric method for determination of oxidized and reduced glutathione in tissues, *Anal. Biochem.* 74 (1976) 214–226.
- K. Winkler, S.A. Altenhoefer, P.W. Kleikers, K.A. Radermacher, C. Kleinschnitz, H. H. Schmidt, VAS2870 is a pan-NADPH oxidase inhibitor, *Cell. Mol. Life Sci.* 69 (2012) 3159–3160.
- A. Daiber, M. August, S. Baldus, M. Wendt, M. Oelze, K. Sydow, A.L. Kleschov, T. Munzel, Measurement of NAD(P)H oxidase-derived superoxide with the luminol analogue L-012, *Free Radical Biol. Med.* 36 (2004) 101–111.
- M. He, R.C. Siow, D. Sugden, L. Gao, X. Cheng, G.E. Mann, Induction of HO-1 and redox signaling in endothelial cells by advanced glycation end products: a role for Nrf2 in vascular protection in diabetes, *Nutr. Metabol. Cardiovasc. Dis.* 21 (2011) 277–285.
- K.M. Robinson, M.S. Janes, M. Pehar, J.S. Monette, M.F. Ross, T.M. Hagen, M. P. Murphy, J.S. Beckman, Selective fluorescent imaging of superoxide in vivo using ethidium-based probes, *Proc. Natl. Acad. Sci. U. S. A.* 103 (2006) 15038–15043.

- [35] D.J. Rowlands, S. Chapple, R.C. Siow, G.E. Mann, Equol-stimulated mitochondrial reactive oxygen species activate endothelial nitric oxide synthase and redox signaling in endothelial cells: roles for F-actin and GPR30, *Hypertension* 57 (2011) 833–840.
- [36] T. Mukaide, Y. Hattori, N. Misawa, S. Funahashi, L. Jiang, T. Hirayama, H. Nagasawa, S. Toyokuni, Histological detection of catalytic ferrous iron with the selective turn-on fluorescent probe RhoNox-1 in a Fenton reaction-based rat renal carcinogenesis model, *Free Radic. Res.* 48 (2014) 990–995.
- [37] M.J. Smith, M. Fowler, R.J. Naftalin, R.C.M. Siow, UVA irradiation increases ferrous iron release from human skin fibroblast and endothelial cell ferritin: consequences for cell senescence and aging, *Free Radical Biol. Med.* 155 (2020) 49–57.
- [38] S. Choi, S. Park, G.H. Liang, J.A. Kim, S.H. Suh, Superoxide generated by lysophosphatidylcholine induces endothelial nitric oxide synthase downregulation in human endothelial cells, *Cell. Physiol. Biochem.* 25 (2010) 233–240.
- [39] T.L. Place, F.E. Domann, A.J. Case, Limitations of oxygen delivery to cells in culture: an underappreciated problem in basic and translational research, *Free Radical Biol. Med.* 113 (2017) 311–322.
- [40] D.C.J. Ferguson, G.R. Smerdon, L.W. Harries, N.J.F. Dodd, M.P. Murphy, A. Curnow, P.G. Winyard, Altered cellular redox homeostasis and redox responses under standard oxygen cell culture conditions versus physioxia, *Free Radical Biol. Med.* 126 (2018) 322–333.
- [41] D.G. Lyons, A. Parpaleix, M. Roche, S. Charpak, Mapping oxygen concentration in the awake mouse brain, *Elife* 5 (2016).
- [42] P.J. Ratcliffe, J.F. O'Rourke, P.H. Maxwell, C.W. Pugh, Oxygen sensing, hypoxia-inducible factor-1 and the regulation of mammalian gene expression, *J. Exp. Biol.* 201 (1998) 1153–1162.
- [43] P.J. Ratcliffe, HIF-1 and HIF-2: working alone or together in hypoxia? *J. Clin. Invest.* 117 (2007) 862–865.
- [44] B. Haas, S. Chrusciel, S. Fayad-Kobeissi, J.L. Dubois-Rande, F. Azuaje, J. Boczkowski, R. Motterlini, R. Foresti, Permanent culture of macrophages at physiological oxygen attenuates the antioxidant and immunomodulatory properties of dimethyl fumarate, *J. Cell. Physiol.* 230 (2015) 1128–1138.
- [45] A.Y. Abramov, A. Scorziello, M.R. Duchen, Three distinct mechanisms generate oxygen free radicals in neurons and contribute to cell death during anoxia and reoxygenation, *J. Neurosci.* 27 (2007) 1129–1138.
- [46] T. Kahles, R.P. Brandes, NADPH oxidases as therapeutic targets in ischemic stroke, *Cell. Mol. Life Sci.* 69 (2012) 2345–2363.
- [47] L. Villeneuve, L.M. Tiede, B. Morsey, H.S. Fox, Quantitative proteomics reveals oxygen-dependent changes in neuronal mitochondria affecting function and sensitivity to rotenone, *J. Proteome Res.* 12 (2013) 4599–4606.
- [48] R. McCormick, T. Pearson, A. Vasilaki, Manipulation of environmental oxygen modifies reactive oxygen and nitrogen species generation during myogenesis, *Redox Biol* 8 (2016) 243–251.
- [49] B. Kalyanaraman, V. Darley-Usmar, K.J. Davies, P.A. Dennery, H.J. Forman, M. B. Grisham, G.E. Mann, K. Moore, L.J. Roberts 2nd, H. Ischiropoulos, Measuring reactive oxygen and nitrogen species with fluorescent probes: challenges and limitations, *Free Radical Biol. Med.* 52 (2012) 1–6.
- [50] H.J. Forman, O. Augusto, R. Brigelius-Flohe, P.A. Dennery, B. Kalyanaraman, H. Ischiropoulos, G.E. Mann, R. Radi, L.J. Roberts 2nd, J. Vina, K.J. Davies, Even free radicals should follow some rules: a guide to free radical research terminology and methodology, *Free Radical Biol. Med.* 78 (2015) 233–235.
- [51] M.P. Murphy, K.S. Echtay, F.H. Blaikie, J. Asin-Cayuela, H.M. Cocheme, K. Green, J.A. Buckingham, E.R. Taylor, F. Hurrell, G. Hughes, S. Miwa, C.E. Cooper, D. A. Svistunenko, R.A. Smith, M.D. Brand, Superoxide activates uncoupling proteins by generating carbon-centered radicals and initiating lipid peroxidation: studies using a mitochondria-targeted spin trap derived from alpha-phenyl-N-tert-butyl-nitron, *J. Biol. Chem.* 278 (2003) 48534–48545.
- [52] J.A. Imlay, Iron-sulphur clusters and the problem with oxygen, *Mol. Microbiol.* 59 (2006) 1073–1082.
- [53] J.P. Ward, Oxygen sensors in context, *Biochim. Biophys. Acta* 1777 (2008) 1–14.
- [54] S.A. Gupte, M.S. Wolin, Relationships between vascular oxygen sensing mechanisms and hypertensive disease processes, *Hypertension* 60 (2012) 269–275.
- [55] E.K. Weir, J. Lopez-Barneo, K.J. Buckler, S.L. Archer, Acute oxygen-sensing mechanisms, *N. Engl. J. Med.* 353 (2005) 2042–2055.
- [56] M. El Alami, J. Vina-Almunia, J. Gambini, C. Mas-Bargues, R.C. Siow, M. Penarrocha, G.E. Mann, C. Borrás, J. Vina, Activation of p38, p21, and NRF-2 mediates decreased proliferation of human dental pulp stem cells cultured under 21% O₂, *Stem Cell Reports* 3 (2014) 566–573.
- [57] R.I. Dmitriev, S.M. Borisov, A.V. Kondrashina, J.M. Pagan, U. Anilkumar, J. H. Prehn, A.V. Zhdanov, K.W. McDermott, I. Klimant, D.B. Papkovsky, Imaging oxygen in neural cell and tissue models by means of anionic cell-permeable phosphorescent nanoparticles, *Cell. Mol. Life Sci.* 72 (2015) 367–381.
- [58] T. Ishii, G.E. Mann, Redox status in mammalian cells and stem cells during culture in vitro: critical roles of Nrf2 and cystine transporter activity in the maintenance of redox balance, *Redox Biol* 2 (2014) 786–794.
- [59] J. Zielonka, J.D. Lambeth, B. Kalyanaraman, On the use of L-012, a luminol-based chemiluminescent probe, for detecting superoxide and identifying inhibitors of NADPH oxidase: a reevaluation, *Free Radical Biol. Med.* 65 (2013) 1310–1314.
- [60] F. Liu, X. Huang, Z. Luo, J. He, F. Haider, C. Song, L. Peng, T. Chen, B. Wu, Hypoxia-activated PI3K/Akt inhibits oxidative stress via the regulation of reactive oxygen species in human dental pulp cells, *Oxid. Med. Cell. Longev.* 2019 (2019) 6595189.
- [61] K. Schroder, NADPH oxidases: current aspects and tools, *Redox Biol* 34 (2020) 101512.
- [62] P. Hernansanz-Agustin, C. Choya-Foces, S. Carregal-Romero, E. Ramos, T. Oliva, T. Villa-Pina, L. Moreno, A. Izquierdo-Alvarez, J.D. Cabrera-Garcia, A. Cortes, A. V. Lechuga-Vieco, P. Jadiya, E. Navarro, E. Parada, A. Palomino-Antolin, D. Tello, R. Acin-Perez, J.C. Rodriguez-Aguilera, P. Navas, A. Cogolludo, I. Lopez-Montero, A. Martinez-Del-Pozo, J. Egea, M.G. Lopez, J.W. Elrod, J. Ruiz-Cabello, A. Bogdanova, J.A. Enriquez, A. Martinez-Ruiz, Na(+) controls hypoxic signalling by the mitochondrial respiratory chain, *Nature* (2020), <https://doi.org/10.1038/s41586-020-2551-y>.
- [63] M.M.A. Almutairi, G. Xu, H. Shi, Iron pathophysiology in stroke, *Adv. Exp. Med. Biol.* 1173 (2019) 105–123.
- [64] T. Imai, S. Iwata, T. Hirayama, H. Nagasawa, S. Nakamura, M. Shimazawa, H. Hara, Intracellular Fe(2+) accumulation in endothelial cells and pericytes induces blood-brain barrier dysfunction in secondary brain injury after brain hemorrhage, *Sci. Rep.* 9 (2019) 6228.
- [65] A. Ashraf, J. Jeandriens, H.G. Parkes, P.W. So, Iron dyshomeostasis, lipid peroxidation and perturbed expression of cystine/glutamate antiporter in Alzheimer's disease: evidence of ferroptosis, *Redox Biol* 32 (2020) 101494.
- [66] B.R. Stockwell, J.P. Friedmann Angeli, H. Bayir, A.I. Bush, M. Conrad, S.J. Dixon, S. Fulda, S. Gascon, S.K. Hatzios, V.E. Kagan, K. Noel, X. Jiang, A. Linkermann, M. E. Murphy, M. Overholtzer, A. Oyagi, G.C. Pagnussat, J. Park, Q. Ran, C. S. Rosenfeld, K. Salnikow, D. Tang, F.M. Torti, S.V. Torti, S. Toyokuni, K. A. Woerpel, D.D. Zhang, Ferroptosis: a regulated cell death nexus linking metabolism, redox biology, and disease, *Cell* 171 (2017) 273–285.
- [67] P. Biemond, H.G. van Eijk, A.J. Swaak, J.F. Koster, Iron mobilization from ferritin by superoxide derived from stimulated polymorphonuclear leukocytes. Possible mechanism in inflammation diseases, *J. Clin. Invest.* 73 (1984) 1576–1579.
- [68] E.T. Chouchani, V.R. Pell, E. Gaude, D. Aksentijević, S.Y. Sundier, E.L. Robb, A. Logan, S.M. Nadtochiy, E.N.J. Ord, A.C. Smith, F. Eyassu, R. Shirley, C.-H. Hu, A.J. Dare, A.M. James, S. Rogatti, R.C. Hartley, S. Eaton, A.S.H. Costa, P. S. Brookes, S.M. Davidson, M.R. Duchen, K. Saeb-Parsy, M.J. Shattock, A. J. Robinson, L.M. Work, C. Frezza, T. Krieg, M.P. Murphy, Ischaemic accumulation of succinate controls reperfusion injury through mitochondrial ROS, *Nature* 515 (2014) 431–435.
- [69] K.M. Holmstrom, L. Baird, Y. Zhang, I. Hargreaves, A. Chalasani, J.M. Land, L. Stanyer, M. Yamamoto, A.T. Dinkova-Kostova, A.Y. Abramov, Nrf2 impacts cellular bioenergetics by controlling substrate availability for mitochondrial respiration, *Biol Open* 2 (2013) 761–770.
- [70] A.T. Dinkova-Kostova, A.Y. Abramov, The emerging role of Nrf2 in mitochondrial function, *Free Radical Biol. Med.* 88 (2015) 179–188.
- [71] T. Ishii, K. Itoh, S. Takahashi, H. Sato, T. Yanagawa, Y. Katoh, S. Bannai, M. Yamamoto, Transcription factor Nrf2 coordinately regulates a group of oxidative stress-inducible genes in macrophages, *J. Biol. Chem.* 275 (2000) 16023–16029.
- [72] Z.A. Shah, R.-C. Li, R.K. Thimmulappa, T.W. Kensler, M. Yamamoto, S. Biswal, S. Doré, Role of reactive oxygen species in modulation of Nrf2 following ischemic reperfusion injury, *Neuroscience* 147 (2007) 53–59.
- [73] R. Penjweini, B. Roarke, G. Alspaugh, A. Gevorgyan, A. Andreoni, A. Pasut, D. L. Sackett, J.R. Knutson, Single cell-based fluorescence lifetime imaging of intracellular oxygenation and metabolism, *Redox Biol* 34 (2020) 101549.
- [74] E. Eroglu, B. Gottschalk, S. Charoensin, S. Blass, H. Bischof, R. Rost, C.T. Madreiter-Sokolowski, B. Pelzmann, E. Bernhart, W. Sattler, S. Hallstrom, T. Malinski, M. Waldeck-Weiermair, W.F. Graier, R. Malli, Development of novel FP-based probes for live-cell imaging of nitric oxide dynamics, *Nat. Commun.* 7 (2016) 10623.
- [75] V.V. Pak, D. Ezerina, O.G. Lyublinskaya, B. Pedre, P.A. Tyurin-Kuzmin, N. M. Mishina, M. Thauvin, D. Young, K. Wahni, S.A. Martinez Gache, A. D. Demidovich, Y.G. Ermakova, Y.D. Maslova, A.G. Shokhina, E. Eroglu, D.S. Bilan, I. Bogeski, T. Michel, S. Vriz, J. Messens, V.V. Belousov, Ultrasensitive genetically encoded indicator for hydrogen peroxide identifies roles for the oxidant in cell migration and mitochondrial function, *Cell Metabol.* 31 (2020) 642–653 e6.